Available online at www.sciencedirect.com
ScienceDirect
International Journal of Heat and Mass Transfer 50 (2007) 2805–2815
International Journal of HEAT and MASS TRANSFER
www.elsevier.com/locate/ijhmt

Interaction of Marangoni convection with mass transfer effects at droplets

B. Arendt, R. Eggers *

Department of Thermal Separation Processes, Heat and Mass Transfer, Hamburg University of Technology, 21071 Hamburg, Germany

Received 16 February 2006; received in revised form 15 August 2006

Abstract

For the system water–acetone–toluene the mass transfer is measured up to a pressure of 200 bar at a constant temperature of 20 °C for two different concentrations at quiescent pendant droplets. The measurements are compared to empirical predictions. The influence of a surfactant is investigated.

A three-mode magnetic suspension balance is used to measure the transfer. Additionally, a Schlieren optic is applied to visualise the convection.

Only in case of the transfer direction from the droplet into the continuous phase Marangoni convection is detected. A good agreement of measurement and evaluation is achieved. The surfactant damps the interfacial convection.

Keywords: Marangoni convection; Mass transfer; Droplet; Surfactant

1. Introduction

Marangoni convection as a transport phenomenon is known for a long time and has ever since provoked the interest of researchers. Especially in recent time increased activities in research regarding interfacial convection [1,2] are noticable.

It is known that Marangoni convection might play an important role in small systems, like thin liquid films and droplets, and that it is the dominant transfer mechanism under zero-gravity conditions [1]. Despite the increased research activities it is still difficult to predict if interfacial convection occurs and to calculate this phenomenon. Especially the interaction of Marangoni convection with other transport phenomena is seldom considered and investigated.

From our former work [3] it is known that it is possible to calculate the mass transfer at a quiescent flat liquid–liquid interface by the linear superposition of free and Marangoni convection. Since first preliminary experiments indicated that the equations used cannot be transferred easily to other geometries in this work the mass transfer at quiescent pendant droplets is examined. The measurements are compared to a calculation based on equations for the mass transfer coefficient found in the literature. Furthermore, the decisive property for Marangoni convection, the interfacial tension, is measured simultaneously to the mass transfer. A Schlieren optic is additionally applied to visualise the mass transfer and detect interfacial convection.

By combining these techniques a deeper insight into the interaction of the different transport phenomena is gained and a possible a priori calculation method is presented.

2. Model equations

2.1. Mass transfer inside droplets

In the literature a variety of equations are found describing the mass transfer into droplets [4]. These theoretical

* Corresponding author. Tel.: +49 40 42878 3191; fax: +49 40 42878 2859.
E-mail address: r.eggers@tu-harburg.de (R. Eggers).
URL: http://www.tu-harburg.de/vt2 (R. Eggers).

0017-9310/$ - see front matter © 2007 Elsevier Ltd. All rights reserved.
doi:10.1016/j.ijheatmasstransfer.2006.10.055

Nomenclature

A	area
B	eigenvalue in Eq. (3)
d	drop diameter
D	diffusion coefficient
L	characteristic length
m	mass
Ma	Marangoni number $\frac{\Delta\sigma L_M}{\eta D}$
n	counting variable
R	enhancement factor
Ra	Rayleigh number $\frac{d^3 g(\rho_{eq}-\rho(t))}{8D\eta}$
Sh	Sherwood number $\frac{\beta L}{D}$
t	time
V	volume

Greek symbols

β	mass transfer coefficient
η	dynamic viscosity
λ	eigenvalue in Eq. (3)
ρ	density
σ	surface tension

Subscripts

A,1	difference between the first measuring point and the zero point
A,2	difference between the second measuring point and the zero point
c	continuous phase
ca	pendant capillary
co	coupling
crit	critical
d	dispersed phase
eq	equilibrium
exp	experimental
i	control variable
j	control variable
M	Marangoni convection
p	partial
ref	reference
s	calculated
SK2	second sinker
tot	total
0	pure dispersed phase

and empirical equations apply for rising or falling drops but most cases are derived for Reynolds numbers smaller than one and, thus, could be applied at quiescent pendant drops. According to the internal flow patterns the models can be divided into three main groups [4]:

- internally stagnant droplets,
- internally circulating droplets,
- oscillating droplets.

For the internally stagnant droplet an equation first found by Gröber [5] reduces to an equation using the solution of the instationary diffusion equation of a sphere [6] if the mass transfer resistance in the continuous phase is neglected. The mass transfer coefficient inside a droplet in case of such a configuration is calculated according to the following equation:

$$\beta_d = -\frac{d}{6t}\ln\left[\frac{6}{\pi^2}\sum_{n=1}^{\infty}\frac{1}{n^2}\exp\left(-\frac{4n^2\pi^2 D_d t}{d^2}\right)\right] \quad (1)$$

in which d stands for the diameter of the droplet, t for the time and D_d for the molecular diffusion coefficient in the drop phase. The equation given above reduces for long contact times by maintaining the first term of the series to

$$\beta_d \simeq \frac{2\pi^2}{3}\frac{D_d}{d} \quad \text{or } Sh_d \simeq 6.58. \quad (2)$$

If internally circulating droplets should be considered Kronig and Brink [7] derived an equation for the calculation of the mass transfer coefficient inside drops for a negligible outside resistance and a Reynolds number much smaller than one ($Re < 0.25$ [8]). Using the stream lines proposed by Hadamard [9] and Rybczyński [10], who applied the Stokes stream function inside and outside a droplet for velocities that small that the quadratic terms can be neglected, Kronig and Brink [7] replaced the physical properties of the two phases by a constant and included this generalized stream function in their further considerations. According to their derivation the following equation was derived:

$$\beta_d = -\frac{d}{6t}\ln\left[\frac{3}{8}\sum_{n=1}^{\infty}B_n^2\exp\left(-\frac{64\lambda_n D_d t}{d^2}\right)\right]. \quad (3)$$

The values for the parameters B_n and λ_n in Eq. (3) are found in the articles by Elzinga and Banchero [11] or Heertjes et al. [12]. Taking only the first term of the series in Eq. (3) into account the equation is reduced for long contact times to a constant Sherwood number:

$$\beta_d \simeq 17.9\frac{D_d}{d} \quad \text{or} \quad Sh_d \simeq 17.9. \quad (4)$$

Alternatively, an approach proposed by Calderbank and Korchinski [13] who introduced an effective diffusivity in the equation for the stagnant drop to account for all internal disturbances, e.g. circulation, can be used. Fitting their experiments gave the following empirical approximation:

$$\beta_d = -\frac{d}{6t}\ln\left[1 - 1 - \exp\left(-\frac{4\pi^2 R D_d t}{d^2}\right)^{\frac{1}{2}}\right]. \quad (5)$$

The enhancement factor R was found to be 2.25. In case of $R = 2.25$ the equation for internally circulating drops found by Kronig and Brink [7] is very well represented. This value for the enhancement factor had been derived from heat transfer measurements in the system gylcerol–bromobenzene. Turning to oscillating droplets two different approaches are found in the literature [4]:

- the surface-stretch model,
- the new surface-elements model.

While in the surface-stretch model it is assumed that all elements stay at the surface during one oscillation cycle and that the surface extension is achieved due to stretching and thinning of the interface, the new surface-elements model proposes that new elements are brought to the interface when the surface increases and that the oldest elements are removed from the phase interface if the surface contracts [4].

Clift et al. [14] stated that both models are notably close to each other. They, moreover, proposed that their equation for the continuous phase mass transfer coefficient can be transferred to the dispersed phase replacing the properties of the continuous phase by those of the dispersed phase. The dispersed phase mass transfer coefficient for oscillating droplets is then estimated by the equation given below [14]:

$$\beta_d = 1.4\frac{\sqrt{D_d}}{d}\left[\frac{48d\sigma}{\pi^2(2\rho_c + 3\rho_d)}\right]^{\frac{1}{4}}. \tag{6}$$

As it has already been mentioned in the introduction in small systems Marangoni convection may play an important role. Since none of the equations above take this phenomenon into account the mechanism will be considered separately in the next section.

2.2. Marangoni convection

For the liquid–liquid extraction a variety of empirical and theoretical equations exists for the mass transfer coefficient under the condition of interfacial convection. Nevertheless, it is still difficult to find a simple equation suitable for chemical engineers which applies for a broad range of systems and geometries, since most of the equations found are restricted to special systems or are of mere theoretical nature [15].

The findings for mass transfer if Marangoni convection occurs lead to the following characterisation [2,15]:

- The mass transfer coefficient is considerably increased due to Marangoni convection.
- The mass transfer coefficient depends on the concentration difference, the properties of the phase interface, like the interfacial tension, and the direction of the transfer.
- In quiescent systems the mass transfer coefficient cannot be described by the penetration theory.
- Above a critical concentration difference the mass transfer coefficient cannot be calculated based on the equation for pure diffusion.

A dimensionless description of the Marangoni effect is achieved by the definition of a Marangoni number.

$$Ma = \frac{\Delta\sigma L_M}{\eta D}. \tag{7}$$

The estimation of the Marangoni number is very difficult since the characteristic length L_M is unknown. Therefore, the integration of this number in model equations is difficult and a further consideration of this number will be omitted in this article.

One of the empirical equations, not using the Marangoni number, starting of the penetration theory derived from the experimental findings of Hozawa et al. [16] was adapted by ourselves and can be used to calculate the mass transfer coefficient at a flat interface due to Marangoni convection separately [3]:

$$\beta_M = \sqrt{\frac{D}{\pi t}}\frac{\sigma_{ref}}{\sigma}. \tag{8}$$

In Eq. (8) D stands for the molecular diffusivity, t for the time and σ for the interfacial tension. For the choice of the reference interfacial tension σ_{ref} two cases are possible and described in our former article in detail [3]:

(1) system without migrating substance and without surfactant;
(2) system without migrating substance with surfactant.

Applying the same equation at curved surfaces like droplets leads to the result shown in Fig. 1.

As it can be seen the mass transfer coefficient for Marangoni convection is overestimated which at first leads to a steep increase in the total transferred mass and afterwards to a decrease. This development is physically impos-

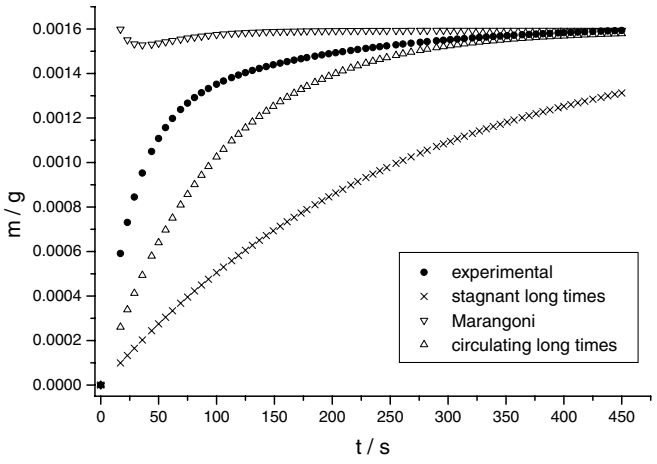

Fig. 1. Temporal development of the CO_2 mass inside a triglyceride droplet at a pressure of 90 bar and a temperature of 20 °C: Marangoni convection calculated with Eq. (8). [17].

sible, thus the equation has to be adapted to suit a wider range of geometries because the experiments conducted by Hozawa et al. [16] were entirely performed at flat interfaces.

Although the dependence of the mass transfer coefficient included in the penetration theory was first suggested by Higbie [18] analysing the mass transfer at droplets the same dependence can be found at a flat interface like falling films [19]. Hence, the first term of Eq. (8) stemming from the penetration theory is maintained in the altered version of the equation for the mass transfer coefficient due to Marangoni convection.

Moreover, according to the knowledge that the driving force for Marangoni convection is the surface tension gradient and that this gradient plays a more important role in systems with an initially small interfacial tension [20] a factor accounting for these facts is introduced into Eq. (8). To keep the model as simple as possible a constant difference in the interfacial tension is chosen which is the difference of the pure system to the system at equilibrium conditions. This constant difference considers the maximal difference in the interfacial tension which could occur at the phase boundary.

Furthermore, Eq. (8) is augmented by the ratio of the hydraulic diameter L_{ref} of the surface equivalent square to the characteristic length of the contemplated geometry, which in case of droplets is the diameter and in case of an arbitrary plate its hydraulic diameter, to broaden the equation to other geometries. Inserting this adoptions into Eq. (8) the following formula, which allows the calculation of the mass transfer due to Marangoni convection separately, is obtained:

$$\beta_{\mathrm{M}} = \sqrt{\frac{D}{\pi t}} \frac{\sigma_{\mathrm{ref}} - \sigma_{\mathrm{eq}}}{\sigma_{\mathrm{ref}}} \frac{L_{\mathrm{ref}}}{L}. \tag{9}$$

The definition of the reference interfacial tension stays like the one for Eq. (8).

3. Materials and experimental set-up

The system water (dispersed phase, *d*)–acetone–toluene (continuous phase, *c*) investigated in this work is the standard test system for the extraction recommended by the European Federation of Chemical Engineering [21]. Acetone and toluene with a purity "pro analysis" (PA $\geqslant$ 99.8%) are used. For the dispersed phase tap water is utilised. For this system the mass transfer is measured for the following conditions:

- different mass transfer direction: $c \rightarrow d$ and $d \rightarrow c$,
- two different initial concentrations of acetone: 7 and 15 wt.%.

Additionally, the influence of the surfactant Triton X-100 (Sigma Chemical) in both phases is determined. The concentration of the tenside in each phase is 0.011 weight percent (wt.%). The influence of the surfactant is only measured for the mass transfer direction $d \rightarrow c$ and the high acetone concentration.

For both systems, the pure and the one containing tenside, the changes of the mass of the water droplet due to the solution of acetone into the droplet or the depletion of acetone in the droplet are measured using the magnetic suspension balance already described in our former article [3]. The exact function of the three mode magnetic suspension balance is described elsewhere [3,22–24]. Since a droplet is to be attached to the suspended system the following changes at the experimental apparatus are carried out, which are shown in Fig. 2.

The first sinker is replaced by a capillary and a mechanism has been developed and is attached to the view cell allowing the movement of a second horizontal capillary. This mechanism moves the collateral capillary towards the hanging one by turning the cap nut. By a pump and a storage vessel a drop is pressed out of the capillary which then connects to the hanging one. Afterwards it is possible to withdraw the collateral capillary by loosening the cap nut again. The piston is then moved outwards by means of the internal pressure.

The apparatus can either be inserted into a lighting–camera–video system or into a Schlieren optic. The former one allows the simultaneous measurement of the changes in mass and interfacial tension. In the latter case the Schlieren optic makes it possible to visualise the mass transfer. The Schlieren optic is described in detail in [25,26].

For the measurement of the interfacial tension the recorded pictures are transferred to a computer and analysed using a commercial software (DSA 1.9, Kruess Hamburg). As a byproduct of the interfacial tension measurements the volume of the drop is calculated which is needed in the calculation of the density (see Eq. (11)).

All experiments are carried out at a constant temperature of 20 °C and at pressures up to 200 bar raising the pressure level in 50 bar steps.

3.1. Density measurement, interfacial tension and mass transfer

Like it has been mentioned in the latter section the measurements are performed using a three-mode magentic suspension balance. The mechanism and the change of the three modes is described in [3].

From a balance of forces at the pendant capillary and the second sinker (see Fig. 2) in both measuring points the density of the droplet and of the continuous phase can be calculated according to the following equations:

$$\rho_{\mathrm{d}}(t) = \frac{m_{\mathrm{A},1} - (m_{\mathrm{co}} + m_{\mathrm{ca}}) + \rho_{\mathrm{c}}(V_{\mathrm{co}} + V_{\mathrm{ca}} + V_{\mathrm{d}})}{V_{\mathrm{d}}} \tag{10}$$

$$\rho_{\mathrm{c}}(t) = \frac{m_{\mathrm{SK2}} + m_{\mathrm{A},1}(t) - m_{\mathrm{A},2}(t)}{V_{\mathrm{SK2}}}. \tag{11}$$

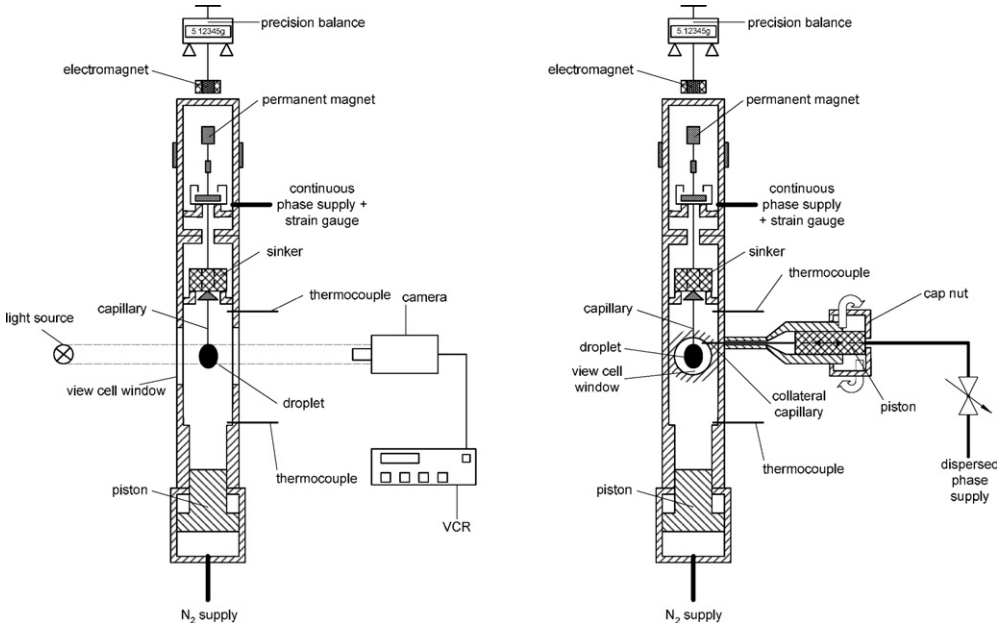

Fig. 2. Experimental apparatus for the mass transfer measurements at a pendant drop.

In Eqs. (10) and (11) ρ stands for the density, m for the mass and V for the volume. The indexes A,1 and A,2 refer to the difference of the mass between the first and the second measuring point, respectively, and the zero point. c denotes the continuous phase, co the coupling, ca the pendant capillary and SK2 the second sinker. As it is described in [3] the mass and the volume of the capillary and the second sinker are extracted from a calibration using a medium of known density.

Measuring the interfacial tension simultaneously gives the volume of the droplet which is inserted into Eq. (11).

Knowing the density and the volume of the drop the partial density $\rho_{p,d}$ and the transferred mass m_{exp} can be calculated according to the functions below:

$$\rho_{p,d}(t) = \frac{\rho_d(t)V(t) - \rho_0 V_0}{V(t)}, \tag{12}$$

$$m_{exp}(t) = \rho_{p,d}(t)V(t). \tag{13}$$

The transferred mass extracted from the measurements in the manner described above is compared to the mass transfer according to the calculation procedure given in the next paragraph.

3.2. Calculated mass transfer

The mass transfer coefficient inside droplets can be described by the models given in Sections 2.1 and 2.2. These models are used to calculated the coefficient separately for each transfer phenomenon, which means that the calculation is conducted separately for each mechanism. In our former article [3] this evaluation procedure has been described in detail and, thus, it is only summarised briefly at this point.

Between a time t_i and t_{i-1} the transferred mass is calculated by

$$m_{i,j}(t_i, t_{i-1}) = \beta A(t_i)\left(\rho_{p,d}(t \to \infty) - \frac{\rho_{p,d,s}(t_i) + \rho_{p,d,s}(t_{i-1})}{2}\right)(t_i - t_{i-1}) \tag{14}$$

and gives as the summation of every time step the transferred mass up to the time t_i

$$m_j(t_i) = \sum_i m_{i,j}. \tag{15}$$

The index i in the equations above denotes a certain time step while the index j stands for a transport mechanism, e.g. internally stagnant droplet or Marangoni convection. If all transport mechanisms have been considered separately the total mass transfer is the sum of all possible mechanisms in such a way that the deviation to the experimental values reduces to a minimum.

$$m_{tot}(t_i) = \sum_j m_j(t_i). \tag{16}$$

In the calculation an estimated partial density $\rho_{p,d,s}$ is introduced.

$$\rho_{p,d,s}(t_i) = \frac{m_{tot}(t_{i-1})}{V(t_i)}. \tag{17}$$

The total mass transferred of the previous time step is used in the estimated partial density to reduce the amount of experimental data needed for the calculation. The disadvantage of this procedure is the introduction of a small mistake using an estimated partial density, although this mistake is very small because of the short time step (one second). Thus, the benefit of no extra experimental data outweighs the disadvantage.

A further simplification of the calculation, which is not pursued at this point, would be to use a constant surface area and volume. Using this very simple procedure would reduce the experimental data needed to a minimum.

4. Results and discussion

For the determination of the main transfer resistance the ratio of the diffusion coefficient in the dispersed phase D_d to the one in the continuous phase D_c must be considered. In case of

$$\frac{D_d}{D_c} < 1, \tag{18}$$

the resistance lies in the dispersed phase and in case of

$$\frac{D_d}{D_c} > 1, \tag{19}$$

the resistance is in the continuous phase [27]. Taking a look at the ratio of the diffusion coefficient of both phases for the different concentrations and transfer directions it is to state that the value of the ratio described above lies in between 0.3 and 0.5. Therefore, the limitation of the mass transfer arises mainly in the dispersed phase. In the following the mass transfer problem will be considered as an internal problem.

4.1. Mass transfer $c \rightarrow d$

A Sterling and Scriven analysis [28] of the system water–acetone–toluene is conducted up-front for this transport direction for both acetone concentrations. In both cases the result of the analysis shows that interfacial convection is not expected, which also means that oscillating convection does not occur.

Furthermore, criteria can be found in literature to calculate the drop diameter at which a droplet starts to oscillate. One of these criteria Klee and Treybal [29] concluded from their experiments in which a droplet falls or rises through another liquid. The critical drop diameter is calculated according to the following equation:

$$d_{crit} = 0.33\rho_c^{-0.14}\Delta\rho^{-0.43}\eta_c^{0.3}\sigma^{0.24}. \tag{20}$$

Using this criterion leads to a critical droplet diameter of 4.1 mm.

Estimating the critical diameter by the formula given by Edge and Grant [30]

$$d_{crit} = 0.162\left(\frac{\rho_d}{\Delta\rho}\right)^{0.5} \tag{21}$$

results in a diameter of 4.5 mm. Since the diameter of the droplets in our investigation varies between 2.5 and 4.4 mm, which is below or near the critical diameter, and since there is almost no external flow an oscillating droplet is not likely to occur.

The density of the droplet is calculated according to Eq. (11) using the volume of the simultaneous interfacial tension measurements. In Fig. 3 the development of the droplet density for a concentration of 7 wt.% in the continuous phase is shown. Additionally, the temporal changes of the interfacial tension is included in the diagram (see Fig. 3).

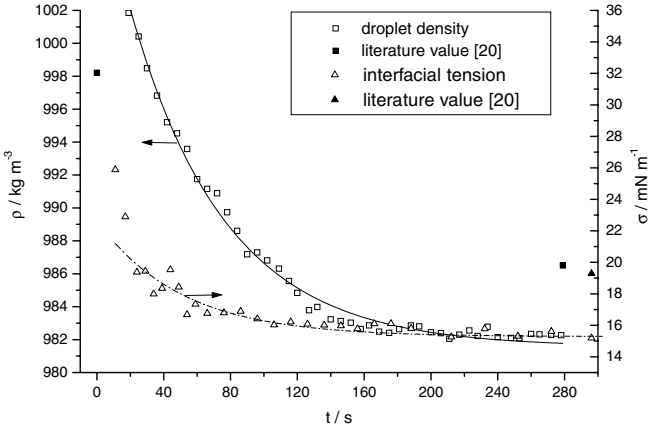

Fig. 3. Temporal development of the droplet density and the interfacial tension at a pressure of 1 bar, a temperature of 20 °C and 7 wt.% acetone in the continuous phase, $d_p = 4$ mm.

The density of the water droplet decreases due to the solution of acetone into the drop. This behaviour has been expected since it is known from literature [21]. The deviation of the measured density to the values found in the literature [21] lies at 0.4%, which is within the experimental accuracy. The same behaviour is noticed at the interfacial tension which also diminishes with time due to the solution of acetone until the equilibrium is reached. The measured interfacial tension at the equilibrium is compared to the interfacial tension taken from the literature [21] at an acetone concentration calculated from the measured density and the partial density. With increasing pressure this behaviour of the density and the interfacial tension stays unaltered.

The transferred mass is then calculated according to the Eqs. (12) and (13) using the measured density and volume. This mass is then compared to the calculation described in Section 3.2. For the mass transfer coefficient β in Eq. (14) the different models mentioned in Sections 2.1 and 2.2 depending whether an internally stagnant droplet, a circulating droplet or Marangoni convection should be considered are utilised. In Fig. 4 the development of the acetone mass inside a water droplet is shown exemplarily at a pressure of 1 bar, a temperature of 20 °C and an initial acetone concentration of 7 wt.% in the continuous phase.

As it can be seen a good agreement of the experimental results and the evaluation is achieved using the model for long contact times by Kronig and Brink [7] which takes an internal circulation into account. Although the model by Kronig and Brink [7] was developed for creeping external flow ($Re < 0.25$ [8]) as the origin of the internal circulation, which we are well aware of, and in this case the mass transfer and as a consequence the change in the density is the reason for the circulation the model by Kronig and Brink [7] is used since no other appropriate model can be

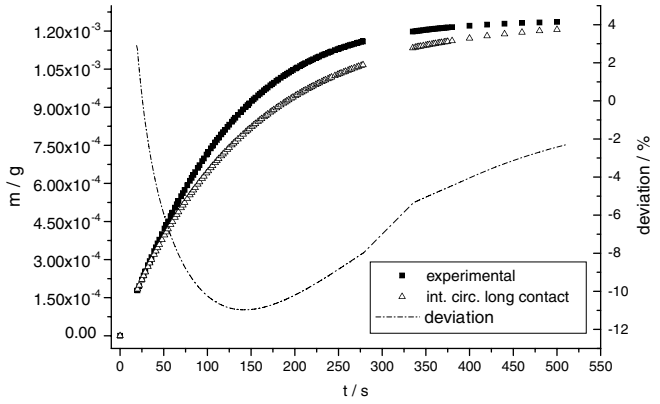

Fig. 4. Temporal development of the acetone mass in a water droplet at a pressure of 1 bar, 20 °C and a continuous phase concentration of 7 wt.%, $d_p = 4$ mm.

found in the literature considering natural convection inside a droplet. In such a model the natural convection should be considered using the Rayleigh number defined as follows:

$$Ra = \frac{d^3 g(\rho_{eq} - \rho(t))}{8D\eta}. \quad (22)$$

The values of the Rayleigh number vary for this configuration at the begining between 4×10^5 and 2×10^6.

That an internal circulation or natural convection occurs can be explained by the change of the density due to dissolving acetone. If acetone is transferred from all sides into the drop the density first reduces at the phase boundary. This also takes place at the bottom of the droplet and as a consequence lighter parts start to ascend. Due to continuity reasons other parts have to flow towards the phase boundary and a circulation pattern builds up.

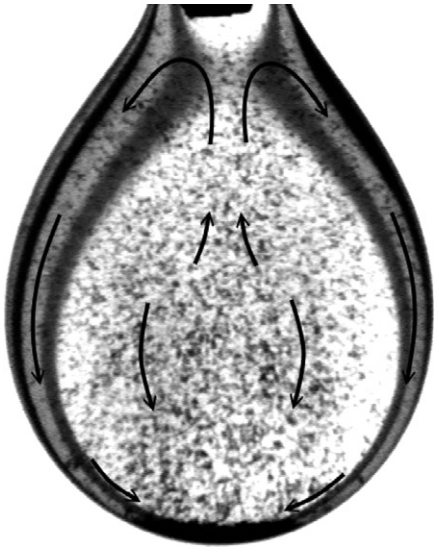

Fig. 5. Profile of the flow pattern in a water droplet in a CO_2 surrounding at a pressure of 160 bar and a temperature of 20 °C.

Since the circulation pattern is similar to the one used in the derivation by Kronig and Brink [7] (see Fig. 5), who used the geometry of the Stokes stream function in the droplet and replaced the physical properties by a constant factor, it seems reasonable to use this model for a circulation pattern of similar geometry. The circulation pattern shown in Fig. 5 has been detected in a different system which has the same density properties with regard to the behaviour if another substance dissolves into it. From this findings it could be assumed that the model by Kronig and Brink [7] could be extended to the limiting case of diminishing external flow.

Another possibility would be to introduce enhancement factors starting of the undisturbed system in which the mass transfer consists of pure diffusion. In this case, comparing Eqs. (2) and (4), the enhancement factor would be 2.72. In general we do not prefer this approach since enhancement factors summarize all effects in a single factor and the role of different effects is blurred.

The agreement of the experimental results and the calculation remains at the same quality if the pressure as well as the concentration in the continuous phase is increased. The temporal development of the experimental results and the calculation in case of an initial concentration of 15 wt.% and a pressure of 100 bar is shown in Fig. 6.

The finding that no interfacial convection occurs in this direction of mass transfer agrees with the analysis according to Sternling and Scrive [28] and is supported by the Schlieren pictures in which Marangoni convection is not visible. Additionally, oscillation is not noticed in the experiments which also agrees with the Sternling and Scriven [28] analysis and the analysis of the critical drop diameter which has been performed at the beginning of this section.

Moreover, these findings agree with the observation by Lewis [31] who also did not detect interfacial convection. More recent studies of the system water–acetone–toluene state that Marangoni convection occurs for the transfer direction templated in this section [2,32,33]. However, this

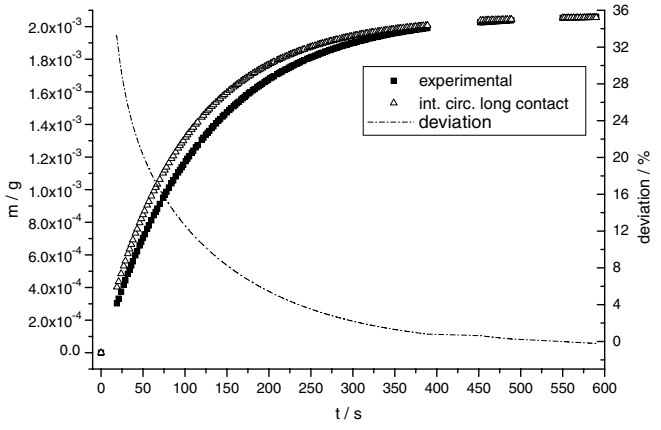

Fig. 6. Temporal development of the acetone mass in a water droplet at a pressure of 100 bar, 20 °C and a continuous phase concentration of 15 wt.%, $d_p = 3.2$ mm.

investigations cannot be compared directly to our investigations since a flat interface and in most cases also moving phases are considered. Concluding from the comparison it seems obvious that the relative movement of the phases has an influence on the occurence of Marangoni convection.

4.2. Mass transfer $d \rightarrow c$

As in the inverse transport direction a Sternling and Scriven [28] analysis is also performed for the transfer direction from the dispersed phase to the continuous phase up-front showing that for both concentrations, 7 and 15 wt.%, stationary but no oscillating interfacial convection is to be expected.

The critical diameter at which a droplet starts to oscillate stays at the value calculated in Section 4.1 leading to the expectation that oscillation does not occur.

The density of the droplet is calculated as for the inverse transfer direction according to Eq. (11) using the volume of the simultaneous interfacial tension measurements. The development of the density and the interfacial tension is exemplarily shown in Fig. 7. The deviation to the literature values lies in between 2% and 3.5%. The deviation of the surface tension at the equilibrium, as it is described in the previous section, is 6.3%.

The density as well as the interfacial tension increases with time due to the depletion of acetone inside the droplet as it has been known from the literature [21].

In case of the transferred mass, calculated according to Eqs. (14)–(16) and compared to the evaluation, it can be seen that a good agreement is achieved using the linear superposition of the mass transfer coefficient for an internally circulating droplet at long contact times and the one for Marangoni convection according to Eq. (9). The problem of the applicability of the model by Kronig and Brink [7] has been discussed in the previous section. The model is used here for the same reasons. Fig. 8 shows the development of the acetone mass inside the droplet at a pressure of 1 bar, a temperature of 20 °C and an initial concentration of 7 wt.%.

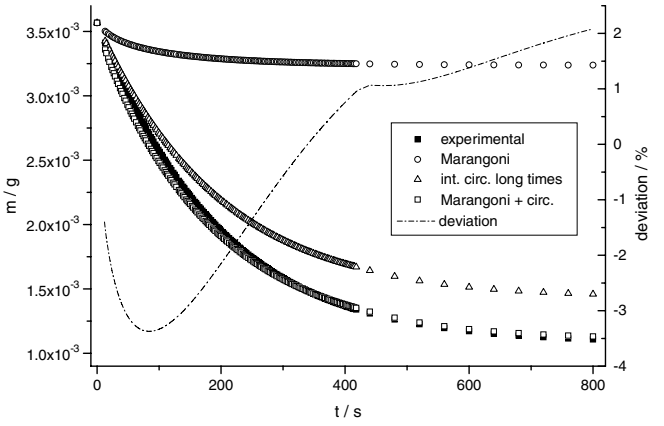

Fig. 8. Temporal development of the acetone mass in a water droplet at a pressure of 1 bar, 20 °C and an initial dispersed phase concentration of 7 wt.%, $d_p = 4.7$ mm.

The agreement of the experimental results and the calculation of the same quality is maintained with increasing pressure and concentration using the equations mentioned above. This can be seen in Fig. 9 which shows the temporal development of the acetone mass inside the droplet at a pressure of 100 bar, a temperature of 20 °C and an initial concentration of 15 wt.%.

If the approach of enhancement factors should be followed the factor to describe circulation and Marangoni convection would be 3 and 3.6 for an initial concentration of 7 and 15 wt.%, respectively. The value of the enhancement factor compared to pure diffusion conditions ($Sh = 6.58$) is gained calculating a constant Sherwood number of about 19.8 for the former concentration and 23.5 for the latter one from the experimental mass transfer. Compared with the enhancement factor for pure circulation the factor is about 10% and 32% larger showing the

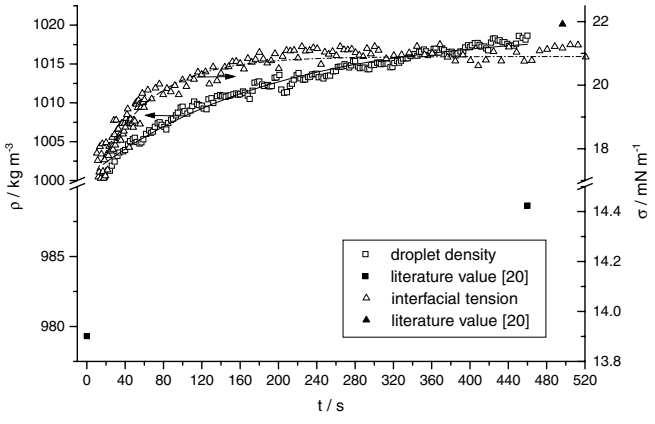

Fig. 7. Temporal development of the droplet density and the interfacial tension at a pressure of 1 bar, a temperature of 20 °C and an initial concentration of 15 wt.% acetone in the dispersed phase, $d_p = 4.3$ mm.

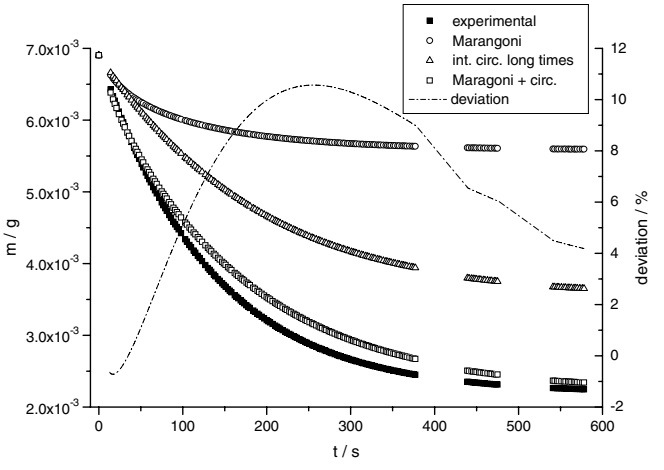

Fig. 9. Temporal development of the acetone mass in a water droplet at a pressure of 100 bar, 20 °C and a initial dispersed phase concentration of 15 wt.%, $d_p = 4.4$ mm.

influence of interfacial convection increasing the mass transfer. Nevertheless, the enhancement factor is a lump sum of both mechanisms making it impossible to distinguish the contribution of the different phenomena. Therefore, this approach is not recommended and not followed at this point.

Concluding from our findings it is to state that the mass transfer can be calculated by the model of an internally circulating droplet at long contact times superimposed by the model for Marangoni convection. Both mechanisms can be estimated separately.

The transfer mechanism Marangoni convection contributes about 15% to the total mass transfer at an initial concentration of 7 wt.%. This proportion is constant with increasing pressure. In case of the higher initial concentration the fraction of Marangoni convection at the total mass transfer increases to almost 27%, again staying constant with increasing pressure.

An increase in the intensity of the interfacial convection with increasing concentration has also been found by Thornton et al. [34]. The existence of interfacial convection and its increase with increasing initial concentration is supported by the Schieren pictures, which show that the intensity decreases with time and can hardly be seen after 90 seconds (see Fig. 10). Moreover, the end of the mass transfer due to Marangoni convection matches the point at which no longer any interfacial convection is seen in the Schlieren pictures (compare Figs. 8 and 9 with Fig. 10).

The rapid decay with time has also been noticed by Thornton et al. [34].

Furthermore, our results are in accordance with the Sternling and Scriven [28] analysis and the results of other researchers who also found Marangoni convection for this direction of mass transfer [2,32,33]. Finally, it is to mention that oscillation has not been detected in the experiments which has been predicted by the analysis of Sternling and Scriven [28] and the calculation of the critical droplet diameter.

4.3. Influence of a surfactant

Due to the fact that only in the direction of mass transfer from the droplet into the continuous phase the existence of Marangoni convection is found, just for this direction the influence of a tenside on the mass transfer at the high initial concentration is investigated.

The density of the droplet is calculated as it has already been described in the last two sections and exemplarily the development of the density and the interfacial tension with time in case of the presence of a surfactant is shown in Fig. 11. As it can be seen in Fig. 11 the interfacial tension of the system is significantly lower than in the pure system due to the presence of the surfactant (compare Figs. 11 and 7). The slightly higher density is due to the experimental error, since the small percentage of the tenside does not influence the density. However, it can be seen that the temporal development and the relative increase in the density is similar (see Figs. 11 and 7). The deviation of the measured density to the one of the pure system is about 5%, which is about the same order of magnitude as in the pure system and a mere consequence of the experimental mistake.

Comparing the experimental mass transfer with the calculation gives the same result as in the latter section. A linear superposition of Marangoni convection and the model by Kronig and Brink [7] leads to a good resemblance of the experimental results. This behaviour does not change with increasing pressure. Fig. 12 shows the changes of the acetone mass inside a droplet exemplarily.

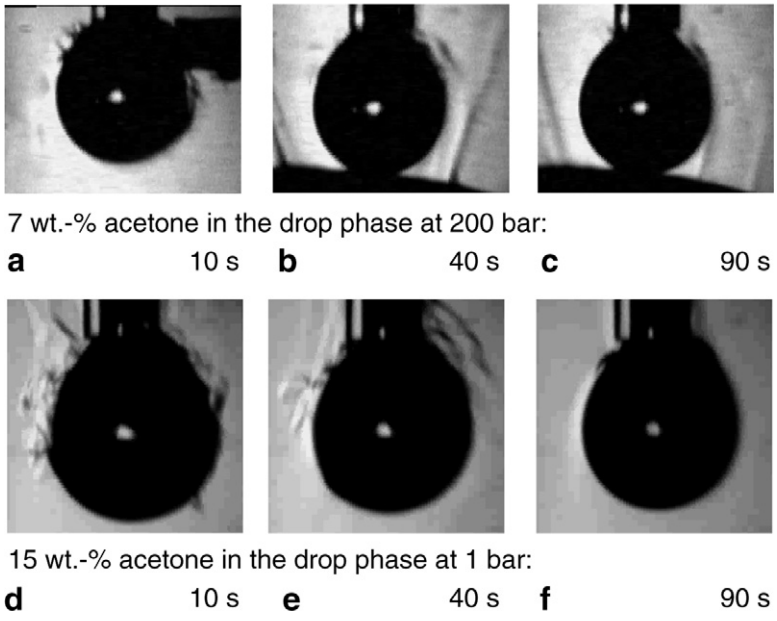

Fig. 10. Schlieren pictures for the mass transfer direction $d \rightarrow c$ in the pure system.

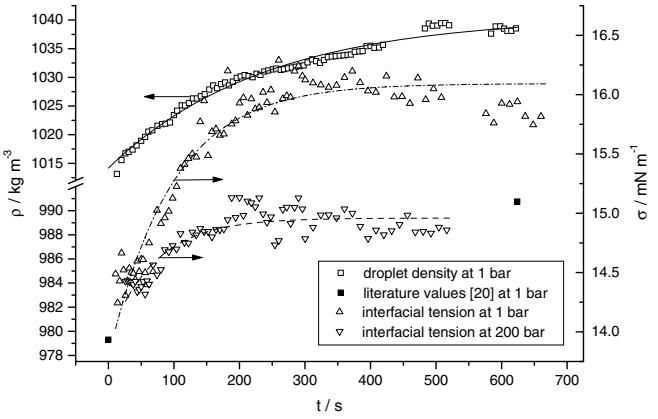

Fig. 11. Temporal development of the droplet density and the interfacial tension at a pressure of 1 bar, a temperature of 20 °C and an initial concentration of 15 wt.% acetone in the dispersed phase in the system containing tenside, $d_p = 3.6$ mm.

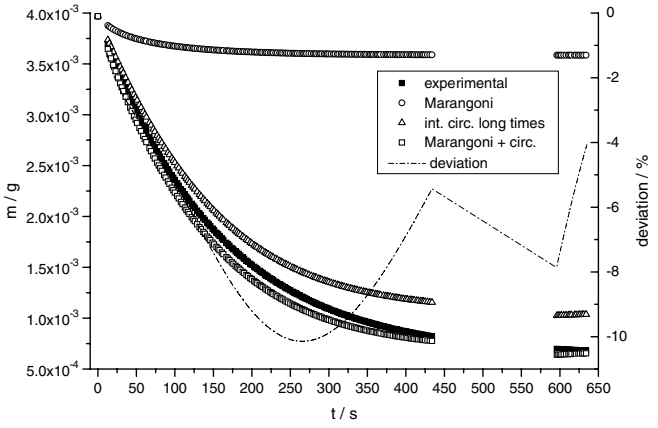

Fig. 12. Temporal development of the acetone mass in a water droplet at a pressure of 1 and 200 bar, 20 °C and an initial dispersed phase concentration of 15 wt.% in the system containing a surfactant, $d_p = 3.6$ mm.

Compared to the mass transfer in the pure system the amount of transferred mass due to Marangoni convection is reduce to 10% of the total mass. This can be explained by the ability of surfactants to damp interfacial convection. The surfactant adsorbs at the interface and a surfactant monolayer is build up leading to an interface which is much less flexible than the one in the pure system [20]. Agble and Mendes-Tatsis [20], moreover, found that especially nonionic surfactants, such as Triton X-100, show a greater tendency to adsorb at the interface and, thus, provoke a more rigid interface preventing interfacial convection. That the interfacial convection is damped can also be seen at the Schlieren pictures in which hardly any interfacial convection is noticeable. From an engineering point of view and if an error of less than 20% is sufficient it is also possible to calculate this transfer situation solely with the model by Kronig and Bring for long contact times [7]. This can also be seen comparing the enhancement factor for the contaminated system which is about 2.85 with the one for pure circulation ($R = 2.72$). The slight increase of only 4.8% shows that it might be sufficient to use the model for internal circulation solely.

5. Conclusions

The mass transfer in the system water–acetone–toluene has been measured for the two possible directions of transfer at two different initial concentration differences, 7 and 15 wt.%.

In case of the transfer from the droplet into the continuous phase the influence of a surfactant on the mass transfer has been investigated for the high concentration difference.

Concluding from the experiments for the transfer direction from the continuous phase into the droplet it can be stated that for both concentrations interfacial convection does not occur. This finding is supported by the Schlieren pictures and agrees with the analysis by Sternling and Scriven [28]. Oscillation has not been visuable which coincides with the analysis according to Sternling and Scriven [28] and the criterion for the beginning of droplet oscillation by Klee and Treybal [29] and Edge and Grant [30]. Moreover, it is possible to calculate the mass transfer for the templated transport direction using the model for long contact times developed by Kronig and Brink [7]. A good agreement of the experimental results and the calculation is achieved with an error of less than 15%.

The model by Kronig and Brink [7] has been used, although the circulation pattern which is used in the original derivation is caused by creeping external flow ($Re < 0.25$ [8]), since a similar circulation pattern has been found in a system behaving like the one contemplated in this article and no other appropriate model describing natural convection inside a droplet can be found in the literature. The natural convection can be expressed in terms of the Rayleigh number which is of the order of 0.5×10^5–2×10^6. The results using this model suggest that it is a good approach and allows the assumption that the model can be extended to the limiting case of vanishing external flow.

The idea of enhancement factors has also been picked up in this article and values are given making it possible to calculate the mass transfer. Nevertheless, this approach is not recommended from our point of view since different phenomena cannot be considered separately. All effects are subsumed in a single factor.

For the inverse direction of the mass transfer, from the droplet into the continuous phase, Marangoni convection is found for both concentration differences which can also be seen in the Schlieren pictures. Furthermore, the mass transfer can be calculated for each transport mechanism separately and the linear superposition of the model for long contact times by Kronig and Brink [7] and the proposed equation for Marangoni convection leads to a good resemblance of the experimental results by the calculation. An error of less than 10% is gained. These findings agree with the prediction by Sternling and Scriven [28] and with the results of other researchers. In addition, an oscillating

droplet has not been detected which has been predicted by the Sternling and Scriven analysis [28]. The criterion for the beginning of droplet oscillation by Klee and Treybal [29] and Edge and Grant [30] of drops falling or rising in another liquid has been applied and shows that the droplet diameter is below or near the critical one which suggested that no oscillation would occur since no extraneous forces due to a flow exist. This is in accordance with our findings.

In case of the presence of a surfactant the interfacial convection is damped due to the higher rigidity of the interface [34]. Nevertheless, it is possible to estimate the mass transfer using the linear superposition of the two models mentioned in the last paragraph. The amount of mass transferred by Marangoni convection reduces from 27% of the total mass transfer in the pure system to 10% in the contaminated system.

From an engineering point of view it might be sufficient to calculate the mass transfer in case of the presence of a surfactant using the model by Kronig and Brink [7].

Acknowledgement

The financial support by the German Research Community (DFG), Project DFG EG 72/22-1, is gratefully acknowledged by the authors.

References

[1] J. Betz, Strömung und Wärmeübergang bei thermokapillarer Konvektion an Gasblasen, Herbert Utz Verlag Wissenschaft, München, 1997.
[2] S. Wolf, Phasengrenzkonvektionen beim Stoffübergang in Flüssig-Flüssig-Systemen, Reihe 3, Nr. 584, VDI Verlag, Düsseldorf, 1999.
[3] B. Arendt, D. Dittmar, R. Eggers, Interaction of interfacial convection and mass transfer effects in the system CO_2–water, Int. J. Heat Mass Transfer 47 (2004) 3649–3657.
[4] A. Kumar, S. Hartland, Correlations for prediction of mass transfer coefficients in single drop systems and liquid–liquid extraction columns, Trans IchemE 77 (Part A) (1999) 372–384.
[5] H. Gröber, Die Erwärmung und Abkühlung einfacher geometrischer Körper, Z. Ver. Dtsch. Ing. 69 (1925) 705–711.
[6] J. Crank, The Mathematics of Diffusion, second ed., Clarendon Press, Oxfort, 1975.
[7] R. Kronig, J.C. Brink, On the theory of extraction from falling drops, Appl. Sci. Res. A2 (1950) 142–154.
[8] M. Stieß, Mechanische Verfahrenstechnik I, second ed., Springer, Berlin, 1995.
[9] J. Hadamard, Mouvement permanent lent d'une sphre liquide et visqueuse dans un liquide visqueux, C.R. Hebd. Seances Acad. Sci. 152 (1911) 1735–1738.
[10] W. Rybczynski, ber die fortschreitende Bewegung einer flssigen Kugel in einem z hen Medium, Bull. Int. Acad. Sci. Cracovie Ser. A (1991) 40–46.
[11] E.R. Elzinga, J.T. Banchero, Film coefficients for heat transfer to liquid drops, Chem. Eng. Prog. Symp. Ser. 55 (1959) 149–161.
[12] P.M. Heertjes, W.A. Holve, H. Talsma, Mass transfer between isobutanol and water in a spray-column, Chem. Eng. Sci. 3 (1954) 122–142.
[13] P.H. Calderbank, I.J. Korchinski, Circulation in liquid drops: a heat transfer study, Chem. Eng. Sci. 6 (1956) 65–78.
[14] R. Clift, J.R. Grace, M.E. Weber, Bubbles, Drops and Particles, Academic Press, New York, 1978.
[15] A.A. Golovin, Interfacial turbulence and mass transfer at liquid/liquid extraction, I. Chem. E. Sympos. Series 119 (1990) 313–326.
[16] M. Hozawa, N. Komatsu, N. Imaishi, K. Fujinawa, Interfacial turbulence during the physical absorption of carbon dioxide into non-aqueous solvents, J. Chem. Eng. Jpn. 17 (2) (1984) 173–179.
[17] B. Arendt, R. Eggers, Interaction of interfacial convection and mass transfer effects in liquid–liquid systems, in: Third International Berlin Workshop on Transport Phenomena with Moving Boundaries, 6th–7th October, 2005, Berlin, Germany, ISBN 3-00-017322-6.
[18] H.D. Baehr, K. Stephan, Heat and Mass Transfer, Springer, Berlin, Heidelberg, New York, 1998.
[19] R.B. Bird, W.E. Stewart, E.N. Lightfoot, Transport Phenomena, John Wiley & Sons Inc., New York, 2002.
[20] D. Agble, M.A. Mendes-Tatsis, The prediction of Marangoni convection in binary liquid–liquid systems with added surfactants, Int. J. Heat Mass Transfer 44 (2001) 1439–1449.
[21] European Federation of Chemical Engineering, Standard Test System for Liquid Extraction, second ed., E Publications Series 46, 1985.
[22] A. Docter, H.-W. Lösch, W. Wagner, Entwicklung und Aufbau einer Anlage zur simultanen Messung der Viskosität und der Dichte fluider Stoffe, Fortschritt-Berichte der VDI-Zeitschriften, Reihe 3, Nr. 494, VDI-Verlag, Düsseldorf, 1997.
[23] H.-W. Lösch, Entwicklung und Aufbau von neuen Magnetschwebewaagen zur berührungsfreien Messung vertikaler Kräfte, Fortschritt-Berichte der VDI-Zeitschriften, Reihe 3, Nr. 138, VDI-Verlag, Düsseldorf, 1987.
[24] R. Kleinrahm, W. Wagner, Entwicklung und Aufbau einer Dichtemeanlage zur Messung der Siede- und Taudichten reiner fluider Stoffe auf der gesamten Phasengrenzkurve. Fortschritt-Berichte der VDI-Zeitschriften, Reihe 3, Nr. 92, VDI-Verlag, Düsseldorf, 1984.
[25] F. Mayinger, O. Feldmann, Heat and Mass Transfer: Optical Measurement Techniques and Applications, Springer, Berlin, Heidelberg, New York, 2001.
[26] G.S. Settles, Schlieren and Shadowgraph Techniques: Visualizing Phenomena in Transparent Media, Springer, Berlin, Heidelberg, New York, 2001.
[27] W.J. Plöcker, H. Schmidt-Traub, Instationarer Stofftransport zwischen einer Einzelkugel und einer ruhenden Umgebung, Chemie-Ing.-Techn. 44 (1972) 313–319.
[28] C.V. Sternling, L.E. Scriven, Interfacial turbulence: hydrodynamic instabilities and the Marangoni effect, AIChE J. 5 (1959) 514–523.
[29] A.J. Klee, R.E. Treybal, Rate of rise or fall of liquid drops, AIChE J. 2 (1956) 444–447.
[30] R.M. Edge, C.D. Grant, Chem. Eng. Sci. 25 (1971) 1001.
[31] J.B. Lewis, The mechanism of mass transfer of solutes across liquid–liquid interfaces. Part II: The transfer of organic solutes across solvent aqueous phases, Chem. Eng. Sci. 3 (1957) 260–278.
[32] H. Christ, Grenzflächenkonvektion unter 1 g- und μg-Bedingungen, Dissertation, Technische Universitaet Berlin, 1987.
[33] M. Pertler, M. Häberl, W. Rommel, E. Blass, Mass transfer across liquid-phase boundaries, Chem. Eng. Pro. 34 (1995) 269–277.
[34] K.H. Javed, J.D. Thornton, T.J. Anderson, Surface phenomena and mass transfer rates in liquid–liquid systems. Part 2, AIChE J. 7 (35) (1989) 1125–1136.